

# EXACT 3D CONE-BEAM RECONSTRUCTION FROM PROJECTIONS OBTAINED OVER A WOBBLE TRAJECTORY ON A C-ARM

K. Ramamurthi and J. L. Prince \*

Johns Hopkins University  
Electrical and Computer Engineering  
Baltimore, MD 21218

N. Strobel<sup>†</sup>

Siemens Medical Solution  
Stanford University Medical Center  
Department of Radiology  
Stanford, CA 94305

## ABSTRACT

We propose a source trajectory for cone-beam geometry that satisfies the conditions for exact 3D reconstruction in the largest sphere that remains non-truncated in the field of view of a given source detector combination. The source trajectory is a natural variation of the traditional circular source trajectory and is achieved by modulating the elevation of the source from the equatorial plane. We use a shift variant filtering approach in developing a filtered back-projection algorithm for robust, and computationally efficient volumetric reconstruction. The method is theoretically exact, and we show some results based upon simulation studies using a mathematical phantom.

## 1. INTRODUCTION

Exact reconstruction in cone-beam geometry has been an exciting topic of research in the last few decades. The theoretical contributions have been mainly two fold. One in laying down the sufficient and necessary conditions on the source trajectory [1, 2]; and the other in actually providing the solution for solving this complex inverse problem [1, 3, 4, 5, 6, 7].

With the advent of multi-row detectors in CT scanners, these theories have been extensively exploited to yield exact multi slice reconstruction using helical trajectories [7, 8, 9, 10]. With C-arms however (such a trajectory being unnatural) there have been other suggestions like a circle and a line [11], two orthogonal circles [6], etc. While a helix is a natural extension of a circle (since it requires only an additional translation), this is not so with these suggested trajectories. This is primarily why there has not been a natural development towards practical algorithms for exact reconstruction in C-arms. Though circular trajectories do not satisfy the conditions for exact reconstruction, armed with the computational simplicity of filtered back-projection algorithms

(like Feldkamp et al, [12]), they continue to dominate the world of C-arms.

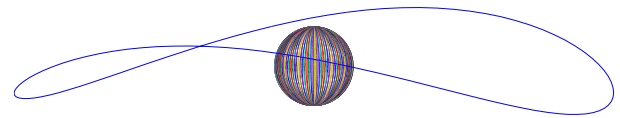


Fig. 1. The wobble trajectory

In this paper, we suggest a source trajectory for exact reconstruction that is a natural extension of the circle. Keeping in mind the ability of C-arms (especially the ceiling mounted ones) to perform rotation about a combination of at least two perpendicular axes we chose to restrict the trajectory onto the surface of a sphere. We suggest that while the source rotates about a fixed axis in a circular fashion, it should also simultaneously *wobble* up and down (see Fig. 1) about another perpendicular moving axis. In order to invert the projections, we adapt the theory of Defrise et al [5] to this specific geometry. While this approach maintains the attractive feature of the filtered back-projection architecture it allows us to exactly reconstruct any region bounded by the largest sphere centered at the iso-center that would fit inside the cone of a given source detector system.

## 2. BACKGROUND

The condition for exact reconstruction in cone-beam tomography (Tuy's principle, [1]) requires that every plane passing through the object support intersect the source trajectory at least once. It also requires that the projections remain non-truncated within the field of view (FOV) of the imaging system. For a source trajectory that is composed of a single continuous segment, Chen proposed the following. The region that can be exactly reconstructed includes that part of the object support that lies within the convex hull of the source trajectory [2]. This follows naturally from Tuy's

\*Thanks to Siemens Corporate Research for funding.

<sup>†</sup>The third author performed the work while at Erlangen, Germany

principle. We refer to such source trajectories as being *complete*.

There have been many methods proposed that can provide exact reconstruction from complete trajectories. These can be broadly classified into two kinds: (i) re-binning algorithms, (ii) filtered back-projection type algorithms. The re-binning class of algorithms involve filling up an intermediate function related to the 3D Radon transform of the object, as suggested by Grangeat [3] and Smith [4], followed by inversion of this function to obtain the reconstruction. The filtered back-projection (FBP-type) algorithms have a simpler architecture (similar to that of approximate methods like Feldkamp et al, [12]) that makes them preferable over the first kind. Kudo et al, [6] and Defrise et al [5] proposed a shift-variant filtering approach by unifying Grangeat's and Smith's theory. The most recent advance in reconstruction theory being a truly shift invariant FBP approach as shown by Katsevich [7] for application in helical CT.

There have also been many suggestions for complete trajectories that employ one of the methods mentioned above for specific applications in SPECT, helical CT etc. Zeng et al [11] employed Smith's method for a circle and orthogonal line geometry that was suitable for SPECT imaging. Various methods have also been proposed in helical CT that solve the long object problem and deal with axial truncation [7, 8, 9, 13]. Unfortunately, the application of exact reconstruction theory in C-arm reconstructions has been relatively unpopular. It is our goal in this paper to both present a trajectory capable of exact reconstruction and demonstrate a practically efficient method.

### 3. METHODS

#### 3.1. The Wobble Source Trajectory

In this section we describe the wobble trajectory. We use the notion of a virtual planar detector that is located at a fixed distance  $D$  (focal length) from the source. The width of the detector is given by the angle it subtends at the source, also known as the cone angle  $\beta$ . The source detector normal defines the origin of reference that always lies on the virtual detector. The orientation of the detector is thus entirely dependent on the source position, which is in turn given by (see Fig. 2),

$$\mathbf{a}(\lambda) = D \cos \lambda \cos \tau \hat{\mathbf{x}} + D \sin \lambda \cos \tau \hat{\mathbf{y}} + D \sin \tau \hat{\mathbf{z}}$$

$$\text{where, } \tau(\lambda) = \frac{\beta}{2} \sin(2\lambda) \text{ and } \lambda \in [0, 2\pi] \quad (1)$$

Here, the trajectory is entirely parameterized by the scalar  $\lambda$  while the elevation of the source from the central plane ( $z = 0$ ) is  $\tau$ . The modulation of  $\tau$  causes the source to *wobble* above and below the equatorial plane. Given a fixed cone angle  $\beta$ , and fixed focal length  $D$ , it is easy to show

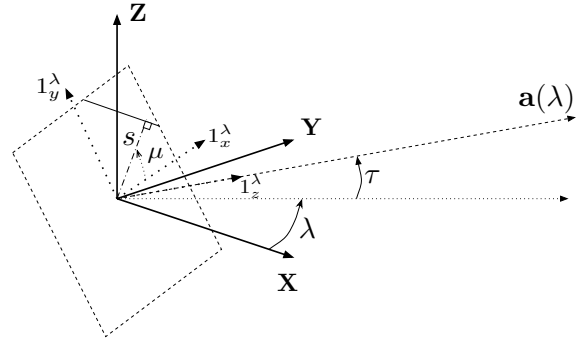


Fig. 2. The source detector geometry

that the largest sphere that remains non-truncated at the iso-center has a radius  $r_D = D \sin(\frac{\beta}{2})$ . It can be shown that the convex hull of this source trajectory entirely includes this sphere.

#### 3.2. Shift Variant Filtered Back-Projection

We use the method described by Defrise et al [5] for the purpose of inversion. For a more detailed explanation of the intermediate functions please refer to [5]. Let the projected image from a source point  $\mathbf{a}(\lambda)$  be given by  $g(x, y, \lambda)$ . Then using the notations as depicted in Fig. 2, the reconstruction formula is given by,

$$f(\mathbf{x}) = \int_0^{2\pi} d\lambda \frac{1}{|\mathbf{x} - \mathbf{a}(\lambda)|} g^F(x, y, \lambda) \quad (2)$$

where,  $\mathbf{x} \in R^3$ ,  $|\mathbf{x}| \leq r_D$  and the filtered projection  $g^F(x, y, \lambda)$

$$= (x^2 + y^2 + D^2) \int_0^\pi d\mu \left( \frac{\partial S_1(s, \mu, \lambda)}{\partial s \sqrt{s^2 + D^2}} \right)_{s=x \cos \mu + y \sin \mu} \quad (3)$$

where  $s$  and  $\mu$  are the sinogram coordinates in the image plane, and  $S_1(s, \mu, \lambda)$  is an intermediate function given by

$$S_1(s, \mu, \lambda) = \frac{-1}{4\pi^2} M(s, \mu, \lambda) \left| \mathbf{a}'(\lambda) \cdot \hat{\theta}(s, \mu, \lambda) \right| S(s, \mu, \lambda) \quad (4)$$

where  $\hat{\theta}(s, \mu, \lambda)$  is the unit normal of the plane that passes through the source position  $\mathbf{a}(\lambda)$  and intersects the image plane on the line  $(s, \mu)$ .  $S(s, \mu, \lambda)$  is related to the projected image as follows,

$$S(s, \mu, \lambda) = \frac{s^2 + D^2}{D^2} \left( \frac{\partial}{\partial s} R(g_1)(s, \mu, \lambda) \right) \quad (5)$$

where,  $R(g_1)(s, \mu) =$

$$\iint dx dy \frac{Dg(x, y, \lambda)}{\sqrt{x^2 + y^2 + D^2}} \delta(s - x \cos \mu - y \sin \mu) \quad (6)$$

The algorithm is implemented by tracing these steps backwards. Eq. (6) is merely the sinogram of the scaled projection. This sinogram is then differentiated and scaled in (5). The intermediate function evaluated in (4) consists of a couple of trajectory dependent terms that we will evaluate in the next section. The intermediate function is then scaled and differentiated once more before being back-projected onto the 2D image plane, giving the shift-varying filtered projection in (3). The filtered projections are then simply 3D back-projected appropriately to yield the reconstruction in (2).

### 3.3. Evaluation of Trajectory Dependent Terms

Let  $(1_x^\lambda, 1_y^\lambda, 1_z^\lambda)$  define the orthogonal co-ordinate system of a detector pose for a given source position  $\mathbf{a}(\lambda)$ . From (1) it can be shown that

$$1_x^\lambda = -\sin \lambda \hat{\mathbf{x}} + \cos \lambda \hat{\mathbf{y}} \quad (7)$$

$$1_y^\lambda = -\cos \lambda \sin \tau \hat{\mathbf{x}} - \sin \lambda \sin \tau \hat{\mathbf{y}} + \cos \tau \hat{\mathbf{z}} \quad (8)$$

$$1_z^\lambda = \cos \lambda \cos \tau \hat{\mathbf{x}} + \sin \lambda \cos \tau \hat{\mathbf{y}} + \sin \tau \hat{\mathbf{z}} \quad (9)$$

and using Eq. (27) in [5], we get

$$\hat{\theta} = (D \cos \mu 1_x^\lambda + D \sin \mu 1_y^\lambda + s 1_z^\lambda) / \sqrt{s^2 + D^2} \quad (10)$$

Using Eqs. (1,7-10), it can be shown that

$$\mathbf{a}(\lambda) \cdot \hat{\theta} = \frac{Ds}{\sqrt{s^2 + D^2}} \quad (11)$$

$$\mathbf{a}'(\lambda) \cdot \hat{\theta} = \frac{D^2 (\cos \tau \cos \mu + \tau' \sin \mu)}{\sqrt{s^2 + D^2}} \quad (12)$$

The intermediate function is hence evaluated as

$$\frac{S_1(s, \mu, \lambda)}{\sqrt{s^2 + D^2}} = -\frac{\tilde{M}(s, \mu, \lambda)}{4\pi^2} \frac{\partial}{\partial s} R(g_1)(s, \mu, \lambda) \quad (13)$$

$$\tilde{M}(s, \mu, \lambda) = M(s, \mu, \lambda) |\cos \tau \cos \mu + \tau' \sin \mu| \quad (14)$$

The weighting function  $M(s, \mu, \lambda)$  is used to handle data redundancy. Consider the plane  $\hat{\theta}(s, \mu, \lambda)$ , that intersects the source trajectory at  $\mathbf{a}(\lambda)$ . If this plane also intersects the source trajectory at various other points, it is necessary to distribute the contributions arising from these simultaneous measurements. It is also necessary for this weight to vanish if the intersection of the plane with the trajectory is tangential at  $\mathbf{a}(\lambda)$ . Such a weighting scheme may be arrived at by using the following expression as suggested in [5]:

$$M(s, \mu, \lambda) = \frac{|\mathbf{a}'(\lambda) \cdot \hat{\theta}(s, \mu, \lambda)|^m c(\lambda)}{\sum_{\alpha=1}^{n(\hat{\theta}, \lambda)} |\mathbf{a}'(\lambda_\alpha) \cdot \hat{\theta}(s, \mu, \lambda)|^m c(\lambda_\alpha)} \quad (15)$$

where  $n(\hat{\theta}, \lambda)$  is the number of solutions for the intersection of the plane  $\hat{\theta}(s, \mu, \lambda)$  with the source trajectory, and  $\lambda_\alpha$  are

the solutions.  $m$  is chosen to be a fixed positive integer. For closed trajectories, (no boundaries)  $c(\lambda)$  may be set to the value 1 everywhere.  $M(s, \mu, \lambda)$  needs to be evaluated over the domain  $\lambda \in [0, 2\pi]$ ,  $\mu \in [0, \pi]$ , and  $s \in [-e, +e]$  where  $e$  is half the length of the main diagonal of the detector. Due to the lack of a closed form expression for the solutions of intersection, a computationally intensive procedure is used for the calculation of the weights. Since this needs to be done only once, it is not of great concern. One can take advantage of the symmetry of the wobble trajectory to show the following

$$\tilde{M}(s, \mu, \lambda) = \tilde{M}(s, \mu, \pi + \lambda) \quad (16)$$

$$\tilde{M}(s, \mu, \lambda) = \tilde{M}(-s, \pi - \mu, \pi/2 + \lambda) \quad (17)$$

$$\tilde{M}(s, \mu, \lambda) = \tilde{M}(s, \pi - \mu, \pi/2 - \lambda) \quad (18)$$

Thus the weights have to be evaluated only over  $\lambda \in [0, \pi/4]$ . The computation of the weights over this range was implemented numerically in the following manner. Given any plane (by specifying  $s, \mu$ , and  $\lambda$ ), solve numerically for all  $\lambda_\alpha$  that satisfy Eq. (11). Corresponding to every source position  $\mathbf{a}(\lambda_\alpha)$ , this plane intersects the detector on a line given by  $(s_\alpha, \mu_\alpha)$ . Comparing the right side of Eq. (11) for different  $\alpha$ 's, it is easy to see that  $s_\alpha = s$ . Observe using Eqs. (7-10) that,

$$\hat{\theta} \cdot \hat{\mathbf{z}} = \frac{s \sin \tau_\alpha + D \sin \mu_\alpha \cos \tau_\alpha}{\sqrt{D^2 + s^2}} \quad (19)$$

Use this equation to evaluate  $\sin \mu_\alpha$  conclusively. In a similar fashion,  $\cos \mu_\alpha$  can be determined by using  $\hat{\theta} \cdot \hat{\mathbf{x}}$  or  $\hat{\theta} \cdot \hat{\mathbf{y}}$ . Finally the overall weighting function  $\tilde{M}(s, \mu, \lambda)$  is evaluated using Eqs. (12,14, and 15)

## 4. RESULTS

For the purpose of simulation we used a mathematical phantom comprising of 7 discs (thickness 10 mm, radius 65 mm) that were stacked axially with their centers 20 mm's apart. The projections were simulated using a software called Take [14] on a square virtual detector (512x512) from a focal length of  $D = 750$  mm and cone angle  $\beta = 15^\circ$ . We ran two sets of experiment, one obtaining projections on a full circle, and the other obtaining projections on the wobble trajectory as described in (1). For the purpose of reconstruction, we used Feldkamp's algorithm [12] to obtain a reconstruction from the projections obtained on a full circle, and used the method described in Sect.3 (using  $m = 4$ ) to obtain a reconstruction from the projections obtained on the wobble trajectory. The back-projection steps were efficiently implemented by using projection matrices [15].

In Fig. 4 we show a central sagittal slice through the original phantom, the Feldkamp reconstruction and our reconstructed volume. The results clearly show that our reconstruction does not suffer from the axial blurring artefact

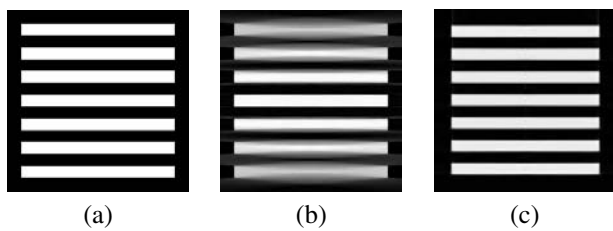


**Fig. 3.** Central sagittal slices of (a) reference phantom; (b) Feldkamp reconstruction from a full circle scan; and (c) Exact reconstruction from wobble trajectory.

that is typical of reconstructions from planar source trajectories. While Feldkamp's algorithm is exact in the central plane, and reasonable for small cone angles, it clearly deteriorates further away from the central plane. Our method, on the other hand shows considerable improvement in the reconstruction of these discs.

## 5. CONCLUSION

We have presented some preliminary results for a non-planar source trajectory that allows us to exactly reconstruct the entire 3D region enclosed within the field of view of any cone-beam geometry. It can be shown that our trajectory satisfies the completeness conditions required for exact reconstruction of such a region. A shift-variant filtered backprojection method has been used for the purpose of reconstruction. We have provided a detailed explanation of how the redundancy weights may be numerically evaluated. The weights need to be evaluated only once, and play a critical role in the *exactness* of the reconstruction.

## 6. REFERENCES

- [1] H.K. Tuy, "An inversion formula for cone-beam reconstruction," *SIAM Journal of Applied Mathematics*, vol. 43, pp. 546–552, 1983.
- [2] J.X. Chen, "A theoretical framework of regional cone-beam tomography," *IEEE Transactions on Medical Imaging*, vol. 11, pp. 342–350, 1992.
- [3] P. Grangeat, "Analyse d'un système d'imagerie 3d par reconstruction à partir de radiographies x en géométrie conique," *Ph.D. thesis, Ecole Nationale Supérieure des Télécommunications*, 1987.
- [4] B.D. Smith, "Image reconstruction from cone-beam projections: Necessary and sufficient condition reconstruction methods," *IEEE Transactions on Medical Imaging*, vol. MI-4, pp. 14–25, 1985.
- [5] M. Defrise and Clack R., "A cone-beam reconstruction algorithm using shift-variant filtering and cone-beam backprojection," *IEEE Transactions on Medical Imaging*, vol. 13, no. 1, pp. 186,194, Mar. 1994.
- [6] H. Kudo and Saito T., "Fast and stable cone-beam filtered backprojection method for non-planar orbits," *Physics in Medicine and Biology*, vol. 43, pp. 747–760, 1998.
- [7] A. Katsevich, "Analysis of an exact inversion algorithm for spiracl cone-beam CT," *Physics in medicine and biology*, vol. 47, pp. 2583–2597, 2002.
- [8] S. Schaller, F. Noo, F. Sauer, K.C. Tam, G. Lauritsch, and T. Flohr, "Exact radon rebinning algorithm for the long object problem in helical cone-beam CT," *IEEE transactions on medical imaging*, vol. 19, pp. 361–375, 2000.
- [9] M. Defrise, F. Noo, and H. Kudo, "A combination of rebinning and exact reconstruction algorithms for helical cone-beam scanning," *The sixth int. meeting on fully three-dimensional image reconstruction in radiology and nuclear medicine, Asilomar*, pp. 98–101, NOV 2001.
- [10] K.C. Tam, S. Samarasekara, and F. Sauer, "Exact cone-beam CT with a spiral scan," *Physics in medicine and biology*, vol. 43, pp. 1015–1024, 1998.
- [11] G.L. Zeng and G.T. Gullberg, "A cone-beam tomography algorithm for orthogonal circle-and-line orbit," *Physics in Medicine and Biology*, vol. 37, pp. 563–577, 1992.
- [12] L.A. Feldkamp, L.C. Davis, and J.W. Kress, "Practical cone-beam algorithm," *Optical Society of America*, vol. 1, no. 6, June 1984.
- [13] K.C. Tam, G. Lauritsch, and K. Sourbelle, "Filtering point spread function in backprojection cone-beam CT and its applications in long object imaging," *Physics in medicine and biology*, vol. 47, pp. 2685–2703, 2002.
- [14] Jens Müller-Merbach, *Manual: Simulation of X-Ray Projections For Experimental 3D Tomography*, 1996.
- [15] N. Navab, A. Bani-Hashemi, M. Nadar, K. Wiesent, P. Durlak, T. Brunner, K. Barth, and R. Graumann, "3d reconstruction from projection matrices in a c-arm based 3d-angiography system," *First International Conference: Medical Imaging Computing and Computer-Assisted Intervention (MICCAI)*, Oct. 1998.